Polar Meteorol. Glaciol., **12**, 58–67, 1998

NORTH-PACIFIC SEA ICE AND KUROSHIO SST VARIABILITY AND ITS RELATION TO THE WINTER MONSOON

Zhifang FANG[1] and John M. WALLACE[2]

[1]*Chengdu Institute of Meteorology, Chengdu, Sichuan, 610041, China*
[2]*Department of Atmospheric Sciences, University of Washington, Seattle, WA 98195, U.S.A.*

Abstract: In this paper, the relationship among large scale patterns of the atmospheric variability, sea-ice concentration and SST over the North-Pacific sector in winter is investigated, making use of the Singular Value Decomposition (SVD) of the temporal covariance matrix. The conclusions are as follows: the main sea-ice pattern over the Pacific sector is comprised of a dipole with opposing centers of action in the Bering Sea and the Sea of Okhotsk. Its temporal variability is strongly related to the atmospheric West Pacific (WP) Pattern, and to the pattern formed in the atmosphere one month earlier than in the sea ice. The WP pattern also affects the SST in the Kuroshio one month later. When the 500 hPa height anomalies are negative over 60°N, 150°E, and positive over 30°N, 150°E, the north part of the East Asian trough is stronger than normal, and the storm track is shifted to the north of its climatic mean position. In the SLP field, the Siberian high and the Aleutian low are weaker than normal, and it is a weak winter monsoon situation in the East Asia. The northerly wind replaces the normal easterly wind over the Sea of Okhotsk, which would be conducive to the advance of the ice edge. The southeasterly wind covers the Bering Sea, which is probably the result of reduced southward transport of sea ice. The northerly wind to the east of Japan in the Pacific is weaker than normal, which would cause positive SST anomalies in the Kuroshio, and *vice versa.*

1. Introduction

The interaction among sea-ice, SST and atmospheric circulation in the climate system is very complicated. Condensation, melting and motion of sea ice cause variability of sea ice concentration, which is obviously related to SST and air temperature. WALSH and SATER (1981) indicated that positive anomalies of SST in the Bering Sea is related to simultaneous negative anomalies of sea ice concentration. The surface wind and the ocean current influence the movement of the ice. As discussed by THORNDIKE and COLONY (1982) and COLONY and THORNDIKE (1984), in the Northern Hemisphere, sea ice tends to drift to the right of the geostrophic wind vector at angles ranging from near 10° to 45°, and its speed and direction are determined by the wind stress.

During winter, atmospheric circulation is stronger both in geostrophic wind and thermal advection. Due to existence of a polar night period in high latitudes, the effect of sea ice on the radiative equilibrium is weaker, and atmospheric circulation forcing on sea ice could play a dominant role. FANG and WALLACE (1993, 1994) indicated that in the North-Atlantic sector the Greenland Blocking affects the sea ice distribu-

tion in the Barents Sea, Greenland Sea and Davis Channel during winter. OVERLAND and PEASE (1982) pointed out that when the cyclone center is located in the southern Bering Sea in winter, then there often exist positive anomalies for sea ice.

There exists a close relationship between SST and atmospheric circulation in the extratropics. LAU (1988) indicated that the WA and WP patterns are accompanied by fluctuations in high frequency baroclinic wave activity, which should influence the oceanic mixed layer. WALLACE *et al.* (1990) have shown that the atmospheric forcing leads the SST response by one month in winter.

CAVALIERI and PARKINSON (1987) noted an out of phase relationship between sea ice cover in the Bering Sea and the Sea of Okhotsk based on a four-winter record of 3-day mean satellite data. Their analysis of a number of specific episodes in which the ice edge advanced in one region and retreated in an other serves to link sea ice anomalies in both regions with the North Pacific Oscillation (NPO), and to demonstrate that sea ice is capable of responding to fluctuations in the atmospheric circulation with time scales on the order of just a few days.

In order to more clearly elucidate the lead-lag relationship among anomalies in sea-ice concentration, SST and related atmospheric fields, we will analyze a data set consisting of monthly sea-ice concentration based on satellite imagery, together with monthly atmospheric and SST data sets. The analysis is restricted to the winter season, when the observed relationships are the strongest.

2. Data and Techniques

The monthly sea-ice concentration anomalies data over the North-Pacific sector based on satellite images were obtained from the US National Snow and Ice Data Center (NSIDC). The data are archived on $2^\circ \times 2^\circ$ grid and cover the Northern Hemisphere poleward of 45°. The record encompasses the period January 1972 through December 1989.

The monthly atmospheric anomalies data for same period as the sea ice data are obtained from the US National Meteorological Center. The data are archived on 445-point Gaussian grid covering the Northern Hemisphere poleward of 20°N.

The monthly SST anomaly data in the North Pacific sector are archived on $4^\circ \times 6^\circ$ grid (latitude interval 4° and longitude interval 6°) in the area 2°–58°N and 120°E–180°–90°W which covers most of the North-Pacific. The data compiled by NCAR, are called the Comprehensive Ocean-Atmosphere Data Set (COADS) data. The period is the same as that coveredly the sea ice data.

The primary analysis tools used in the study are Empirical Orthogonal Function (EOF) and Singular Value Decomposition (SVD) techniques. BRETHERTON *et al.* (1992) introduced the SVD method. WALLACE *et al.* (1992) have discussed the two leading SVD modes of the hemispheric 500 hPa height field and the SST fields over the North Pacific and North Atlantic.

We computed the temporal covariance matrix between normalized sea-ice concentrations at each grid points and SST (or atmosphere data) at each grid points. The output consists of two matrices, the "left" matrix for sea ice and the "right" for SST (or atmosphere data), together with the same number of singular values.

The singular values provide a measure of the squared covariance fraction SCF accounted for by the various singular value vectors. The fraction of the total squared covariance between the two fields accounted for by any mode is proportional to the square of its singular value.

For temporally normalized fields, the singular vectors can be scaled in an analogous manner by multiplying them by the corresponding singular values and dividing by the temporal standard deviation of the expansion coefficient. The maps involve correlations between the expansion coefficients of one field and the grid point values of the other field, as heterogeneous correlation maps.

The correlation coefficient r between the expansion coefficients provides a measure of how strongly the left and right fields are related to one another. The statistical significance of the results can be assessed by comparing the SCF and r values.

3. Climatic Scenario for Sea Ice and SST and Their Interrelationship

FANG and WALLACE (1994) showed that during winter the sea-ice concentration in the Sea of Okhotsk increases from south-east to north-west with the maximum value near the East-Asian coast, while in the Bering Sea it increases from south to north with the maximum value near the Bering Strait; both values are more than 80%. The

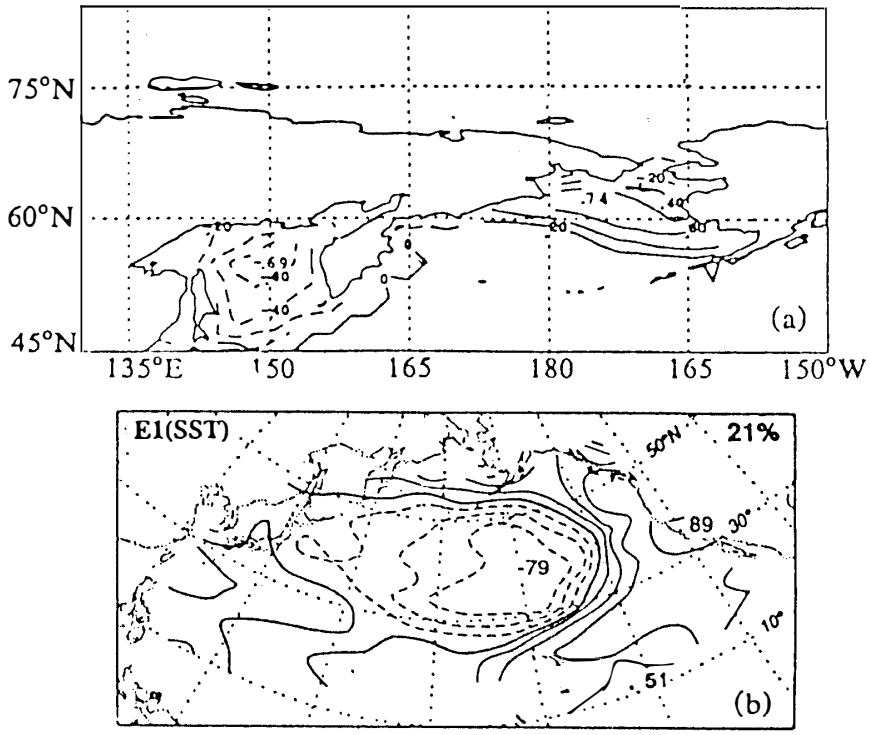

Fig. 1. Horizontal structure of the leading EOFs of the temporal covariance matrix of (a) normalized sea-ice concentration at monthly interval during the winter season for the Pacific sector, and (b) normalized Pacific SST based on data for 39 winter season 1946–1985. The contours show the temporal correlation between the time series of the expansion coefficient of EOF1 and sea ice or SST at each grid point, contour interval is 0.2; negative contours are dashed.

temporal standard deviation of sea ice concentration tends to be large within the Sea of Okhotsk and Bering Sea, exceeding 20% of the climatological mean value in some areas (not shown). Therefore there exist obviously heavy or light sea ice years in the two seas.

Using the EOF method, we analyze the sea-ice variability in the North Pacific sector during winter (January, February and March) based on the data from 1972 to 1989. Figure 1a shows the first EOF mode of normalized sea ice over the North Pacific at monthly intervals, scaled such that the value at each grid point is the correlation coefficient between the time series of the expansion coefficients of the EOF1 and the normalized sea-ice concentration at that point. The horizontal structure of the leading EOF, which accounts for 27% of the total variance, exhibits an out-of-phase relationship between sea ice anomalies in the Bering Sea and the Sea of Okhotsk. The negative correlation extreme value (*i.e.*, −0.69) is located in the Sea of Okhotsk, and the positive extreme value (*i.e.*, 0.74) is located in the Bering Sea. The positions of the correlation center are close to the temporal standard-deviation centers of sea-ice concentration. It is evident that the centers of sea-ice concentration distribution appearing as out-of-phase often occur in areas of obvious sea-ice variability.

The SST variability over the North Pacific in winter has been analyzed by many meteorologists. WALLACE *et al.* (1992) showed the structure of the leading EOF of wintertime SST (Fig. 1b). The negative and positive centers are located in the eastern Pacific at 40°N,160°W and 35°N,130°W respectively, and in the northwestern Pacific the correlations are rather weak. The leading mode accounts for 21% of total SST variance.

Relations between fluctuations in wintertime sea ice concentration and SST over the North Pacific were explored, making use of singular value decomposition (SVD), as described in Section 2. In order to allow for the possibility that the strongest relationships might be observed, not in the simultaneous correlations, but in the correlations with one field lagging by some time interval relative to the other, the analysis was performed for a sequence of different lag intervals. The sea ice fields were fixed in the three winter months (January, February and March, *i.e.*, J.F.M.), while the SST time series were shifted from October, November and December (*i.e.*, O.N.D.) in the previous year to March, April and May (*i.e.*, M.A.M.) for the current year. As a result, the structures of the leading SVD modes for sea-ice and SST in all of the tests are similar, the SCF1s almost equal 60% and the correlation coefficients ($r1$) are near 0.65, which means that the coupled relationship between the sea ice and SST continues throughout the winter half year.

The SVD leading modes between the simultaneous sea ice and SST are shown in Fig. 2. The heterogeneous correlation pattern for the normalized sea ice concentration (Fig. 2a) is similar to the pattern of the leading EOF (Fig. 1a), which represents the most important mode of sea ice distribution in the North Pacific. The SST pattern for the SVD leading mode (Fig. 2b) is very different from the EOF1 mode for the SST (Fig. 1b); there exists an obvious positive center to the east of Japan (*i.e.*, over the Kuroshio area, its value is 0.61, and the positive correlation coefficient center in the East Pacific is weaker than the leading EOF mode for the SST in Fig. 1b. The result indicates that the larger sea-ice concentration over the Sea of Okhotsk often

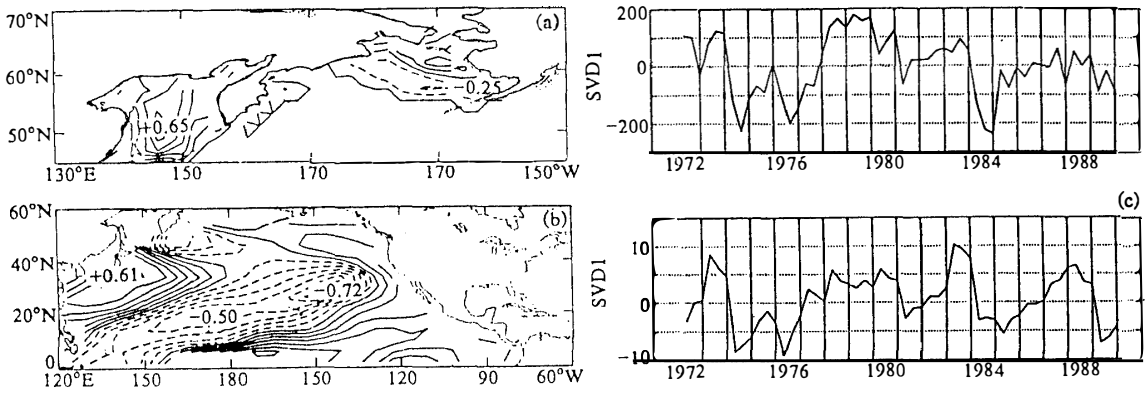

Fig. 2. Heterogeneous correlation patterns for the leading mode derived from SVD of the temporal covariance matrix between wintertime (a) sea-ice concentration and (b) the SST over the North Pacific sector. Contour interval is 0.1; negative contours are dashed. (c) time series of the expansion coefficients for sea-ice and SST derived from the leading SVD mode, the vertical line represent breaks in the time series for year.

has a close relationship with warmer SST in the Kuroshio area throughout the winter half year. The time series of the expansion coefficients for the sea ice and SST are shown in Fig. 2c. Both have a similar tendency, the correlation coefficient is 0.66.

Using the wintertime Kuroshio SST index (the averaged SST over 20°–45°N, 120°–170°E), the simultaneous correlation field between the Kuroshio SST index and the sea-ice concentration in the Pacific sector is very similar to Fig. 2a (figure is omitted).

It may be difficult to explain why large sea-ice concentration in the Sea of Okhotsk is associated with warmer Kuroshio SST to the south near the sea ice area, but they might be relared through the atmospheric circulation. So we will discuss the atmospheric forcing on sea ice and SST separately.

4. The Atmospheric Circulation Related to Sea Ice and SST

The analysis is similar to that in Section 3, but relations between fluctuations in wintertime sea ice concentration and hemispheric 500-hPa height, sea level pressure, and the 1000–500-hPa thickness field were explored, making use of singular value decomposition (SVD). In order to obtain the strongest relationship, the analysis was performed for a sequence of different lag intervals as in Section 3. The sea ice fields were fixed in wintertime, while the atmospheric fields were shifted from October, November and December (O.N.D.) in the previous year to March, April and May (M.A.M.) for the current year. The statistics of the leading modes derived from these calculations are summarized in Table 1.

The squared covariance fraction (SCF) and the correlation coefficient between the time series of the expansion coefficients of the two fields (r) are all measures of the strength of the relationship between the two fields. All three of these indicators reach their peak values with sea ice lagging the atmospheric variables by one month. The relationships are of comparable strength for all three atmospheric fields. For the sake

Table 1. Statistics for the leading mode in the SVD expansion of wintertime sea ice concentrations over the North-Pacific sector at 1-month intervals and the atmospheric 500-hPa height, sea level pressure (SLP), and 1000–500-hPa thickness fields. Lag time is the number of 1-month time steps by which the sea ice data lagged the atmospheric data. SCF is the squared covariance fraction between the two fields explained by the leading mode; r1 is the correlation coefficient between the time series of the expansion coefficients for the leading mode.

	500 hPa		SLP		Thickness	
Lag months	SCF (%)	r1	SCF (%)	r1	SCF (%)	r1
−2	37	0.54	32	0.52	36	0.58
−1	39	0.59	47	0.56	45	0.66
0	42	0.62	43	0.61	50	0.73
1	49	0.73	51	0.73	51	0.76
2	40	0.56	43	0.59	38	0.59
3	38	0.56	34	0.54	37	0.65

of brevity, we will henceforth emphasize the results based on the 500-hPa height field, and we will infer the relationships between sea ice concentration and the sea level pressure and thickness fields indirectly.

The heterogeneous correlation pattern for sea ice, shown in Fig. 3a, is virtually identical to the correlation pattern for the leading EOF of wintertime sea ice over the North-Pacific shown in Fig. 1a, which represents the principal mode of the sea ice field.

The heterogeneous correlation pattern of 500-hPa height are shown in Fig. 3b. There exists a pair of negative and positive centers in the East Asian and Western Pacific area. The negative center is located over eastern Siberia (60°N,150°E) and the positive center is around Japan (38°N,145°E). The pattern resembles the western Pacific pattern (WP), of which WALLACE and GUTZLER (1981) studied the statistical significance of the height distributions at 500 hPa and SLP in the Northern Hemisphere in winter. When this pattern exists, the polar vortex shifts to eastern Siberia, the northern part of the East Asian trough is stronger than normal, and the northern Pacific storm track tends to be shifted to the north of its climatological position, as indicated by LAU (1988). The atmospheric circulation should affect the sea ice distribution. OVERLAND and PEASE (1982) showed that the sea ice anomalies over the Bering Sea may be related to storm track action during winter. Our results agree with them, that is when the cyclonic center was located over the northern Bering Sea, sea ice negative anomalies often appeared in the area.

In order to shed more light on the physical linkages between the sea ice and 500-hPa height patterns, the corresponding SLP pattern in December, January and February for the leading mode derived from SVD is shown in Fig. 3c. According to the pattern of SLP anomalies, the negative center is located over eastern Siberia (65°N,160°E) and the positive center is located east of Japan (42°N,150°E). The pattern resembles the West Pacific Pattern (WP) of SLP, defined by WALLACE and GUTZLER (1981). In this situation, the Siberia High and the Aleutian Low are both weaker than normal, so it is a weak east Asian winter monsoon situation. When this pattern exists, the

(a)

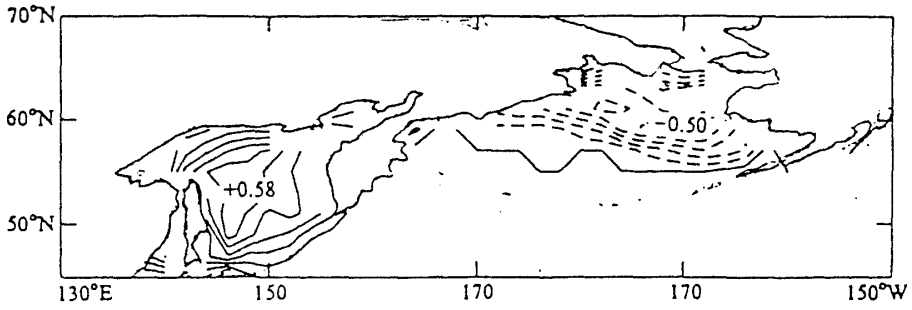
70°N
60°N
50°N
+0.58
-0.50
130°E
150
170
170
150°W

(b)

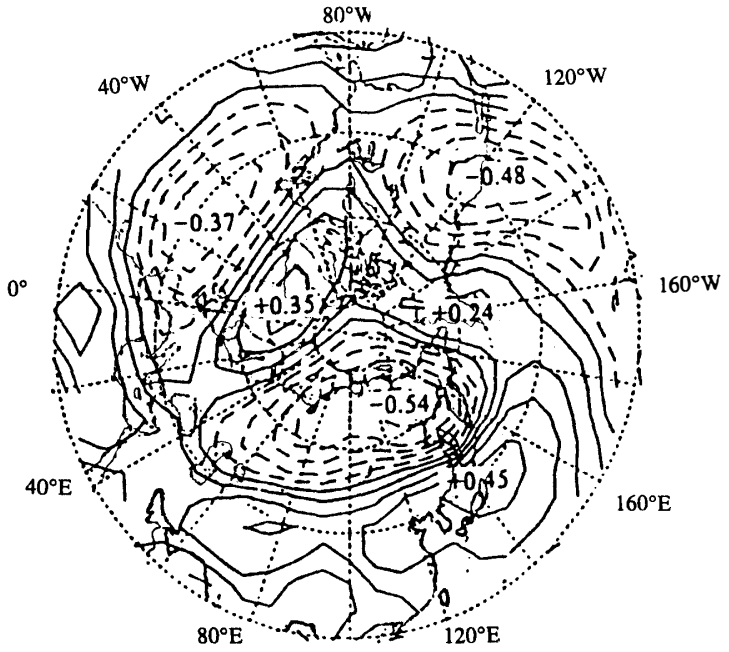
80°W
40°W
120°W
-0.48
-0.37
0°
160°W
+0.35
+0.24
-0.54
40°E
+0.45
160°E
80°E
120°E

(c)

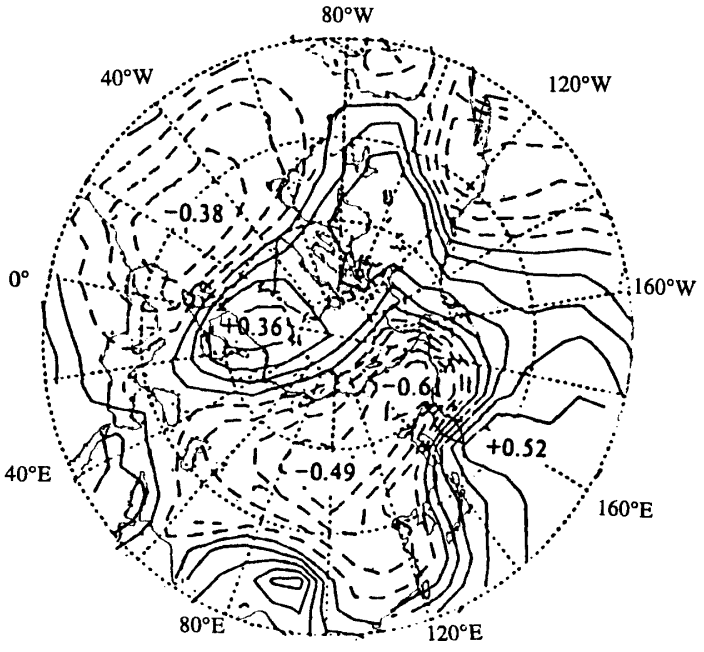
80°W
40°W
120°W
-0.38
0°
160°W
+0.36
-0.61
+0.52
40°E
-0.49
160°E
80°E
120°E

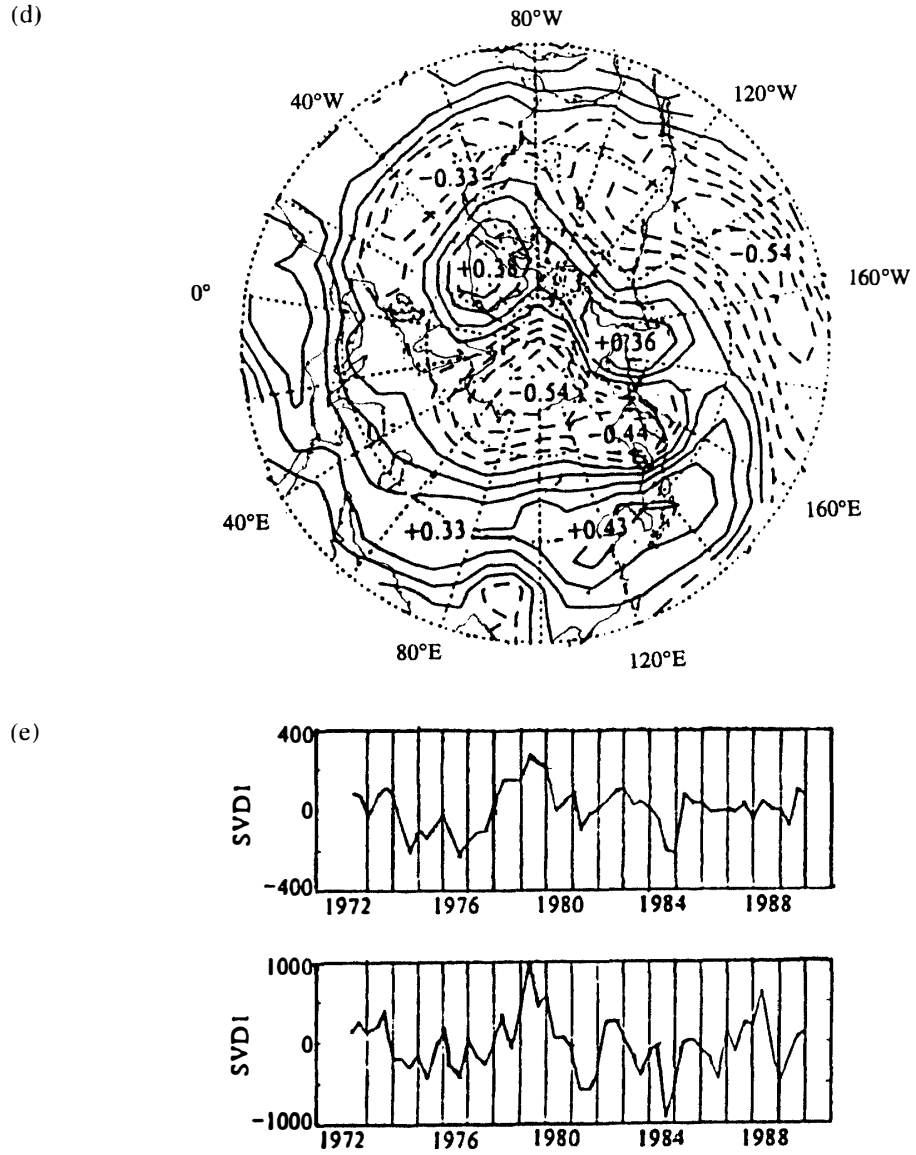

Fig. 3. Heterogeneous correlation patterns for the leading mode derived from SVD of the temporal covariance matrix between (a) wintertime (i.e., J.F.M.) sea ice concentration over the Pacific sector and (b) the hemispheric 500-hPa height field, (c) SLP and (d) 1000–500-hPa thickness. The atmospheric fields are 1 month earlier than sea ice (i.e., D.J.F.). (e) Time series of the expansion coefficients for sea ice concentration and 500-hPa height derived from the leading SVD mode; top is for sea ice and bottom for 500-hPa height.

meridional gradient in isocorrelation is stronger than normal over the Sea of Okhotsk, which indicates that the geostrophic surface wind anomalies over the Sea of Okhotsk should be westerly. The isocorrelations are from southwest to northeast over the Bering Sea, which indicates that the geostrophic surface wind anomalies should be southwesterly there. Our results suggest that sea ice distribution may be influenced by the geostrophic surface wind. Due to sea ice concentration over the Sea of Okhotsk increasing from southeast to northwest and its increase from south to north over the Bering

Sea, as described in Section 3, the wind should advect the ice edge eastward over the Sea of Okhotsk and push the ice edge back northeastward over the Bering Sea, as discussed by THORNDIKE and COLONY (1982) and COLONY and THORNDIKE (1984).

The corresponding 1000–500-hPa thickness pattern in December, January and February for the leading mode derived from SVD is shown in Fig. 3d. The negative and positive centers are located in the Sea of Okhotsk and the Bering Sea, which indicates the consistency between sea ice decrease (increase) and positive (negative) temperature anomalies.

The time series of the expansion coefficients of the sea ice and 500-hPa height field for the leading SVD mode shown in Fig. 3e share a very similar long term tendency. Their correlation coefficient reaches 0.73. The time series of sea ice is similar to that shown in Fig. 2c, and the correlation coefficient between them is 0.91. This shows that the sea ice distribution is closely related to the preceding atmospheric circulation anomalies and simultaneous SST anomalies.

Using the Kuroshio SST index, as defined in Section 3, the relationships between SST index and the hemispheric 500-hPa height, sea level pressure and 1000–500-hPa thickness field are investigated. The Kuroshio SST indexes are fixed to January, February and March, the atmospheric fields were shifted from O.N.D. in the previous year to M.A.M. for the current year. For the atmospheric data from N.D.J. to F.M.A., the correlation patterns are similar to the WP pattern with extreme value position located as in Fig. 3 (not shown), but for O.N.D. and M.A.M., the pattern is not like the WP pattern. The results are summarized in Table 2. All three of these correlation coefficients reach their peak values with atmospheric variability leading the Kuroshio SST by one month. This means that when the winter monsoon was weaker than normal, the Kuroshio SST would have positive anomalies, but the SST anomalies would lag the atmosphere by one month because of the thermodynamic and dynamic adjustment of the ocean. Our results suggest that SST anomalies may be influenced by the geostrophic surface wind. As HANAWA *et al.* (1989) discussed by mean of a composite method, in warm (cold) winter when remarkable positive (negative) SST anomalies appear in mid-latitudes of the western North Pacific, the axis of mid-latitude westerlies moves northward (southward), correspondingly, the easterlies in low lati-

Table 2. The correlation coefficients between the Kuroshio SST index and WP pattern in 500-hPa height, sea level pressure (SLP), and 1000–500-hPa thickness fields. Lag time is the number of 1-month time steps that the SST data lagged relative to atmospheric data. "S.r" and "N.r" mean the correlation coefficients at the grid points (30°N, 150°E) and (60°N, 150°E). "no WP" means that there does not exist a WP pattern in the correlation field map.

	500 hPa		SLP		Thickness	
Lag months	S.r	N.r	S.r	N.r	S.r	N.r
−2	no WP		no WP		no WP	
−1	0.38	−0.36	0.36	−0.41	no WP	
0	0.50	−0.35	0.43	−0.36	0.58	−0.22
1	0.77	−0.46	0.69	−0.47	0.74	−0.38
2	0.57	−0.36	0.66	−0.26	0.60	−0.39
3	no WP		no WP		no WP	

tudes strengthen (weaken) and are associated with change of position of the convection region. With reduction (development) of the Siberian high in a warm (cold) winter, the center of the Aleutian low moves northward (southward). These changes cause those of the WSV (*i.e.*, wind stress vector) fields.

As above, the WP pattern in the atmosphere influences the sea ice distribution in the North Pacific and the SST in the Kuroshio during winter. Because of the thermodynamic and dynamic character of sea ice and SST, so they both lag the atmosphere by one month.

Acknowledgments

We would like to thank Xinhua CHENG and Yuan ZHANG, who advised and assisted in setting up the analysis. Naoto IWASAKA provided helpful comments. This work was supported by the National Science Foundation of China through the study of relationship between sea ice and atmosphere program from 1996 to 1998. This publication also in funded by the Joint Institute for the study of the Atmosphere and Ocean (JISAO).

References

BRETHERTON, C. S., SMITH, C. and WALLACE, J. M. (1992): An intercomparision of methods for finding coupled patterns in climate data. J. Clim., **5**, 541–560.

CAVALIERI, D. J. and PARKINSON, C. L. (1987): On the relationship between atmospheric circulation and sea-ice fluctuations in the sea-ice extents of the Bering and Okhotsk Seas. J. Geophys. Res., **92**, 7141–7162.

COLONY, R. and THORNDIKE, A. S. (1984): An estimate of the mean field of Arctic sea ice motion. J. Geophys. Res., **89**, 10623–10629.

FANG, Z.-F. and WALLACE, J. M. (1993): The relationship between the wintertime blocking over Greenland and sea ice distribution over North Atlantic. Adv. Atmos. Sci., **10**, 453–464.

FANG, Z.-F. and WALLACE, J. M. (1994): Arctic sea ice on a time-scale of weeks and its relation to atmospheric forcing. J. Clim., **7**, 1897–1914.

HANAWA, K., YOSHIKAWA, Y. and WATANABE, T. (1989): Composite analyses of wintertime wind stress of vector fields with respect to SST anomalies in the Western North Pacific and the ENSO events, Part 1: SST composite. J. Meteorol. Soc. Jpn., **67**, 385–400.

LAU, N.-C. (1988): Variability of the observed midlatitude storm tracks in relation to low-frequency changes in the circulation pattern. J. Atmos. Sci., **45**, 2718–2743.

OVERLAND, J. E. and PEASE, C. H. (1982): Cyclone climatology of the Bering Sea and its relation to sea ice extent. Mon. Weather Rev., **110**, 5–13.

THORNDIKE, A. S. and COLONY, R. (1982): Sea ice motion in response to geostrophic winds. J. Geophys. Res., **87**, 5845–5852.

WALLACE, J. M. and GUTZLER, D. S. (1981): Teleconnection in the geopotential height field during the northern hemisphere winter. Mon. Weather Rev., **109**, 784–812.

WALLACE, J. M., SMITH, C. and JIANG, Q.-R. (1990): Spatial pattern of atmosphere-ocean interaction in the North winter. J. Clim., **3**, 990–998.

WALLACE, J. M., SMITH, C. and BRETHERTON, C. S. (1992): Singular value decomposition of wintertime sea surface temperature and 500 hPa height anomalies. J. Clim., **5**, 561–576.

WALSH, J. E. and SATER, J. E. (1981): Monthly and seasonal variability in the ocean-ice-atmosphere system of the North Pacific and North Atlantic. J. Geophys. Res., **86**, 7425–7445.

(Received December 24, 1997; Revised manuscript accepted May 6, 1998)